Nanoscale

Accepted Manuscript

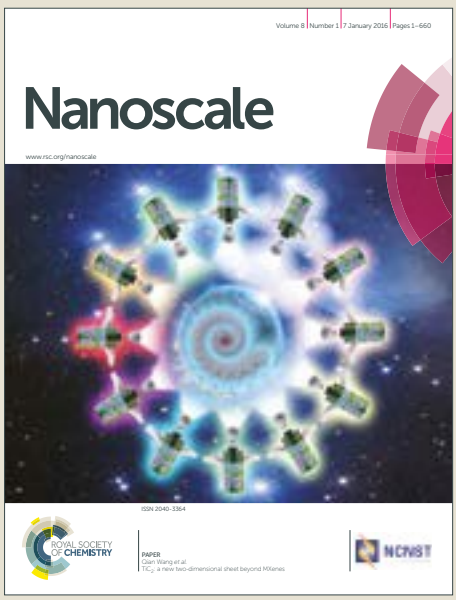

ROYAL SOCIETY OF CHEMISTRY

rsc.li/nanoscale

View Article Online
DOI: 10.1039/C8NR02069H

Supramolecular organization of liquid-crystal dimers - *bis*-cyanobiphenyl alkanes on HOPG by scanning tunneling microscopy†

Klaudyna Krzyżewska,[a] Tomasz Jaroch,[a] Agnieszka Maranda-Niedbała,[a] Damian Pociecha,[b] Ewa Górecka,[b] Ziauddin Ahmed,[c] Chris Welch,[c] Georg H Mehl,[c] Adam Proń,[d] Robert Nowakowski[a]*

[a]Institute of Physical Chemistry, Polish Academy of Sciences, Kasprzaka 44/52, Warsaw 01-224, Poland; [b]Warsaw University, Faculty of Chemistry, Żwirki i Wigury 101, Warsaw 02-089, Poland; [c]School of Mathematics & Physical Sciences, University of Hull, Cottingham Road, Hull, HU6 7RX, UK; [d]Warsaw University of Technology, Faculty of Chemistry, Noakowskiego 3, 00-664 Warsaw, Poland

* Corresponding author. Tel.: +48 22 (0) 343 32 26. Fax: +48 22 (0) 343 33 33; E-mail: rnowakowski@ichf.edu.pl

Keywords: cyanobiphenyl, mesogens, self-organization, scanning tunneling microscopy.

† Electronic supplementary information (ESI) available. See DOI:

2D supramolecular organization of a series of six cyanobiphenyls bimesogens deposited on highly oriented pyrolytic graphite (HOPG) is studied by scanning tunneling microscopy (STM). The adsorbates are 1,ω-bis(4-cyanobiphenyl-4'-yl)alkanes (CBnCB) with different length of their flexible alkyl spacer (containing from 7 to 12 methylene groups). Microscopic investigations at the molecular resolution allow for detailed analysis of the effect of the alkyl spacer length on the type and the

View Article Online
DOI: 10.1039/C8NR02069H

extent of the resulting 2D organization. It has been demonstrated that bimesogens with shorter spacers (7 and 8 methylene units) organize in a similar manner characterized by the formation of two types of differently ordered monolayers: dense packed, wherein the molecules are oriented in one direction and ordered into parallel rows (layer structure), or less dense packed wherein they are organized into a chiral windmill-like structure. For derivatives with longer spacers (ranging from 9 to 12 methylene units) additional effect of parity of carbon atoms in the spacer (even *versus* odd) is observed. In this range of the spacer length even membered bimesogens are still organized in a typical layer structure. However, odd-membered dimers exhibit a much complex 2D supramolecular organization with a larger unit cell and a helical arrangement of the molecules. Careful comparison of this structure with the 3D structural data derived from the X-ray diffraction investigations of single crystals indicates that for these bimesogens a clear correlation exists between the observed complex 2D supramolecular organization in the monolayer and the organization in one of the crystallographic planes of the 3D nematic twist-bent phase.

1. Introduction

Spontaneous organization of organic molecules into highly ordered supramolecular aggregations, frequently called molecular self-assembly, has been the subject of significant research efforts in a wide range of disciplines, including: chemistry, physics, materials science, surface science and biology. These investigations provide information of fundamental importance concerning the distribution of supramolecular interactions in the studied systems and the influence of molecular structure on these interactions. From a practical point of view molecular self-assembly is crucial in all cases where anisotropic arrangements of molecules may lead to direction dependent physical properties such as in active layers in organic electronics.[1] Moreover, in nanotechnology this process is still the most effective way for the fabrication of a wide range of functional nanostructures via the bottom-up approach.

One of the class of organic molecules where there are complex relationships between molecular structure and the resulting supramolecular behavior are mesogens. Self-assembly of these molecules

View Article Online
DOI: 10.1039/C8NR02069H

is generally related to their molecular shape – linear molecules are usually organized into nematic and smectic phases while disc-like molecules preferably assembly in columnar structures - this relationship becomes more complex for molecules that do not have simple rod-like or disc-like shapes. Recently considerable interest in bent-core rigid molecules or bent-core dimers emerged. This is due to the sterically induced packing for polar smectics. Though it has been observed too that these systems also have the unique ability to form short helical pitch nematic and smectic phases (twist-bent nematic phase – N_{TB} or smectic SmC_{TB}) despite being achiral.[2-7] These phase structures, theoretically predicted by Meyer[8] for chiral molecules, and Dozov[9] for achiral bent-core mesogens, are characterized by a periodic twist of the director (preferred direction in a volume element of a molecular orientation) and bend deformation leading to characteristic conical helices. The N_{TB} phase was first described for the liquid crystal dimer 1,ω-bis(4-cyanobiphenyl-4'-yl)heptane (CB7CB) consisting of two cynaobiphenyl mesogenic units linked by a flexible alkyl chain consisting of seven methylene groups.[10] Recently, the same type of organization was also confirmed for other liquid crystal dimers[3,11-16] and trimers,[17,18] as well as bent-core rigid molecules.[19,20] N_{TB} type liquid crystals have been studied using complementary bulk techniques, in particular: freeze-fracture TEM (FFTEM), polarising microscopy, X-ray diffraction (XRD), X-ray scattering (SAXS), anomalous carbon and selenium k-edge scattering, NMR spectroscopy, high magnetic field studies and differential scanning calorimetry.[3-12,21-30] A wide series of properties have been explored including the investigation of the crystallographic properties (with helical pitch determination), correlating the mode of organization with the molecular structure, as well as the theoretical phase structures studies and investigations of the elastic/flexoelastic behavior. The results of such investigations have been summarized recently in a number of reviews.[31-34] Though the bulk properties of the twist-bent phase have been studied in great detail for an increasing number of molecules, the corresponding self-organization of the molecules in two-dimensional systems has not been reported so far. In general, self-assembly is a consequence of mutual non-covalent interactions between neighboring molecules. However, in the case of two-dimensional or low dimensional systems additional effects of molecular interactions with the substrate surface, as well as, different surface phenomena can also occur, leading in some organic systems to observable differences between the 2D and 3D organizations

View Article Online
DOI: 10.1039/C8NR02069H

(polymorphism).[35,36] This correlation is especially interesting for complex supramolecular structures, as observed for the nematic twist-bent phase.

To address the question of similarities and differences in the self-organization of N_{TB} phase forming dimers in two dimensions and the bulk we report the results of our comparative scanning tunneling microscopy (STM) investigations of the two-dimensional organization of six dimers. They are 1,ω-bis(4-cyanobiphenyl-4'-yl)alkanes, where the alkyl spacer has been varied between seven and twelve methylene groups (n=7-12) (abbreviated as CBnCB) on HOPG (model substrate). STM is a surface technique which enables to obtain real-space images with local information (low averaging) at molecular resolution. We focus especially on two important questions (i) concerning the effect of the length of alkyl spacer on the type and the extent of the observed 2D organization, and (ii) the correlation with the corresponding molecular organization in the bulk. Previously, STM investigations have been used to study self-organization in monomolecular layers of alkyl and alkoxy derivatives of cyanobiphenyl monomers on HOPG and MoS_2 substrate surfaces.[37-43] Careful investigations at the molecular resolution enabled to observe and analyze interesting supramolecular phenomena occurring on the surface, such as: dimerization, odd-even effects, and the change of organization and supramolecular interactions caused by the coexistence of molecules with alkyl substituents of different lengths. To the best of our knowledge no STM investigations of any type have ever been reported for cyanobiphenyl dimers separated by alkyl spacers. We report here that these complex molecules exhibit a large range of 2D organizations depending on their chemical constitution. Moreover the data obtained in the surface studies allows us to correlate 2D and 3D structures and connect this with the discussion on the molecular organization in the N_{TB} phase.

2. Experimental section

2.1. Preparation

The synthesis of a series of symmetric dimers, namely 1,ω-bis(4-cyanobiphenyl-4'-yl)alkanes (CBnCB) (n=7-12) was performed according to the methods already described in the literature (Fig.

View Article Online
DOI: 10.1039/C8NR02069H

1a).[3] Additionally, our studies also concern one asymmetric molecule (CB9DFCB) presented in Fig. 1b. This is an asymmetric difluoro-substituted analogue of symmetrical dimer CB9CB from the investigated series. The synthesis of this molecule can be found in the literature.[44, 45] Moreover, the data for the all investigated materials, including 1H and 13C NMR analysis, HPLC and high resolution mass spectrometry data was presented in the Electronic Supplementary Information.

2.2. Modelling

The symmetric molecules consist of two rigid aromatic cyanobiphenyl units connected by a flexible alkyl spacer (Fig. 1a). As the flexible spacers of the dimers are varied by increasing the number of methylene units, the dimension of the studied molecules, along their longitudinal axis in the most extended conformation, vary from 2.95 nm (CB7CB) to 3.6 nm (CB12CB). The values were determined by molecular modeling for a free dimer in the gas phase, as the distance between the two terminal nitrogen atoms on both extremities of the molecules. Here, it is worth to note that the studied dimers have a tendency to exhibit different conformations in the gas phase; this is dependent on the number of carbon atoms in the spacer (even *versus* odd). Taking into account the all-trans conformation of the spacer chain the even membered dimers are of "zigzag" shape in other words over linear, whereas the odd-membered ones are bent (see Fig. 1c, n = 8 and 7, respectively). The width of all molecules (0.43 nm) is determined by the phenyl ring in the stiff segments and corresponds to the distance between the hydrogen atoms at its opposite sides. However, the free dimers are not planar as the two rings in both mesogenic units are mutually tilted. As a consequence, the effective width of the molecule in its adsorbate state can be slightly different to that of the modelled analogue in the gas phase due to spatial orientation of the molecules on the surface or/and molecular deformations caused by adsorbate-substrate interactions.

2.3. STM investigations

View Article Online
DOI: 10.1039/C8NR02069H

The monomolecular layers for microscopic studies were prepared for a given dimer from its solution (1.5 mg L^{-1}) in chloroform (pure, POCh Gliwice (Poland)) by drop casting on a freshly cleaved surface of highly oriented pyrolytic graphite (HOPG, SPI Supplies, USA). Then, after drying under ambient conditions, the samples were imaged in air by means of STM (custom-built setup,[46] University of Bonn, Germany). Images were acquired in a constant-current mode using mechanically cut Pt/Ir (80%/20%) microscopic probes. STM investigations were repeated several times for each dimer at different surface areas and using different samples, to avoid artifacts and get reliable statistical information. The optimal scanning conditions are listed for each case in the corresponding figure caption. The real-space models of 2D organization of the investigated adsorbates on HOPG were postulated by the correlation of the layer structure observed by STM and the van der Waals size and geometry of the molecules (obtained using the HyperChem software package).

3. Results and Discussion

3.1. Dimers with a short spacer (CB7CB, CB8CB)

As evidenced from STM studies of all derivatives, the type of the two-dimensional supramolecular organization on a graphite substrate depends strongly on the alkane spacer length. From this point of view, the investigated dimers can be divided into two groups, those with shorter and longer spacers, as it was found that the spacer length is responsible for inducing a different supramolecular behavior. Molecules with shorter alkane chains, *ie*. having seven or eight methylene groups, exhibit a tendency to self-organize on HOPG in two different ways, depending on the processing conditions. Fig. 2 represents STM images of the dominant organization observed for the CB7CB dimer. This ordering is characterized by parallel rows of molecules oriented in one direction, corresponding to layers in 3D crystals, with a characteristic angle between the molecular tilt and the layer normal equal to 24º (layer structure). This is very similar to values detected for the N_{TB} phase for this systems,[47] and close to that deduced from carbon k-edge experiments.[28] Each dimer is visible as a set of two bright spots separated by ca. 1.4 nm (two molecules are schematically marked on the right side of the image – each molecule is a set of two white cycles (cyanobiphenyl units) linked by a white line (alkyl

View Article Online
DOI: 10.1039/C8NR02069H

spacer)). It is expected that the two bright spots of each molecule are related to the cyanobiphenyl units - areas of higher tunneling current and/or geometrically highest points of the molecule due to non-planar orientation of phenyl rings on the substrate surface. Averaging periodicities observed in this image over a larger area enabled us to determine characteristic molecular distances and to identify the adsorption geometry (Fig. 2b). The layer distance of 2.6 nm, which is significantly smaller than the length of the dimer, indicates that the cyano-end groups of the molecules from the neighboring layers are interdigitated. The most plausible factor which stabilizes such a molecular organization is self-segregation of polar and non-polar molecular fragments or/and a level of hydrogen bonding between the cyano groups and phenyl ring hydrogen atoms (see scheme presented in Fig. 2b1). The second characteristic distance, 0.85 nm, corresponds to the spacing between the adjacent molecules inside the layer and correlates with the width of a dimer molecule and dense packing of cyanobiphenyl units (Fig. 2b). Finally, it is important to note that the basic layer structure is modulated, molecular layers are characterized by a wavy shape. Careful inspection of the obtained images indicates that molecules are grouped into aggregates, each consisting of four molecules (see segments marked by white lines in Fig. 2c). Taking into account this superstructure, the proper crystallographic unit cell of the discussed structure is therefore four times larger along axis *b* as it has to include the whole segment consisting of four molecules. The crystallographic unit cell of the structure is oblique with parameters a = 2.6 nm, b = 3.4 nm, γ = 94º. The basic motive – a four molecule aggregate - is tilted with respect to the crystallographic unit cell side *b* by 6°. The observed structure is the 2D version of so called the broken layer B_{1rev} phase,[48] that has been found for many bent-core molecules but also for bent-dimer mesogens, although the reason for the formation of the planar structures is likely to be different. The likely driving-force for the formation of imperfections in molecular arrangements of organic molecules monolayers on graphite substrate is a misfit between the organizations of the adsorbate layers and the substrate surface. As a consequence the accumulation of strains in the monolayer is expected during the film formation. The strains are minimized by stress relaxation in the layer, realized by the observed additional shift of every fourth molecule in each molecular row. It is interesting to note that the angle between the molecule long axis in the monolayer and the averaged row direction (axis *b*) is ca. 60°. This value correlates well

View Article Online
DOI: 10.1039/C8NR02069H

with the three-fold symmetry of the graphite substrate surface. An analogous effect was also previously observed for cyanobiphenyl monomers[34] and was explained by a difference between the organization of two parts of the molecule, which generates a stress. The alkyl chains are forced to densely pack following the arrangement of carbon atoms on the graphite substrate surface, whereas the cyanobiphenyl units require larger separation due to repulsive interactions between nitrogen atoms of the neighboring molecules in each molecular row.

The layer organization is also observed for the CB8CB dimer. The structure is characterized by parallel rows of bright spots, separated by alternatively occurring darker and brighter zones. Comparison of the monolayer images obtained for CB7CB and CB8CB (Figs 2a and 3b, respectively) shows that the spacer extension leads to broadening of bright zones between the cyanobiphenyl units, confirming that these areas are filled with alkyl chains. The measured crystallographic unit cell parameters: a = 3 nm, b = 1.1 nm, $\gamma = 91°$ indicate that for this homologue too there is slight interdigitation of the terminal cyano groups, resulting in a network of intermolecular hydrogen bonds (Fig. 3).

The layer-like organization is dominant for dimers with shorter alkyl spacers. However, for some samples a different type of assembling mode was observed on a local scale too, with a *windmill shape* motive made of four bright spots arranged in squares. A representative STM image of this new molecular arrangement for CB7CB is presented in Fig. 4a. The unit cell parameters (a = 2.1 nm, b = 2.4 nm, $\gamma = 95°$) together with the results for the adsorption geometry lead us to model for the self-assembly of the systems. Here, each set of four bright spots correspond to a set of four cyanobiphenyl groups, each originating from a different neighboring molecule, mutually linked by a network of hydrogen bonds (Fig. 4b with scheme presented in the bottom-right corner). We emphasize that a critical characteristic of the windmill motive is that it is chiral. A striking feature is the hydrogen boding like interaction with the terminal nitrile groups with the hydrogen groups of the aromatic ring systems. The observed monolayer structures show that non chiral molecules form spontaneously stable supramolecular structures with chiral properties. Surprisingly, the same type of molecular ordering was also observed for an adsorbate with a longer spacer CB8CB (Fig. 4c), where due to the

View Article Online
DOI: 10.1039/C8NR02069H

more linear structure the adoption of bent-shaped conformations was much less expected. The unit cell determined for this longer derivative is slightly larger in both directions (a = 2.3 nm, b = 2.5 nm, γ = 94º) when compared to the corresponding unit cell determined for the shorter CB7CB adsorbate. We note, that images of the windmill-like structure CB8CB were noticeably less resolved than those detected for CB7CB, indicative of the lower stability of this type of molecular assembly. An important feature of the two observed types of self-assembly is the difference of the molecular packing density between the layer and windmill-like organizations with the layer structure being more dense. For CB7CB the corresponding values are: 2.2 nm^2 for the layer structure and 2.5 nm^2 for the windmill-like structure, a difference of about 10%.

3.2. Dimers with long spacers (CB9CB to CB12CB)

Even membered molecules. The longer dimers with an even number of methylene groups (CB10CB, CB12CB) in the spacer are characterized by layer structures as previously described for CB8CB. A comparison of the monolayer images, obtained for CB12CB and its shorter analogue CB8CB (Figs 5 and 3, respectively) confirms that the spacer extension leads to broadening of brighter zones between the cyanobiphenyl groups. The unit cell parameters, determined from STM images are: a = 3.1 nm, b = 1.1 nm and γ =91º; a = 3.35 nm, b = 1 nm and γ = 92°; a = 3.6 nm b = 1 nm and γ = 92º, for molecules with spacers consisting of 8, 10 and 12 methylene groups, respectively. An increase of the spacer length leads to an increase of only the parameter a of the unit cell. This is expected, taking into account that the same type of supramolecular organization is observed and the orientation of the molecules within the layers is similar.

Odd membered molecules. Starting from the spacer containing nine methylene groups the odd membered dimers exhibit a very different supramolecular organization when compared to the even membered analogues. This clearly indicates that the odd-even effect, important in 3D liquid crystalline organization of these molecules, plays too a significant role for monolayers deposited on weakly interacted substrates (like HOPG). Typical STM images of a representative CB9CB monolayer deposited on HOPG are presented in Fig. 6. The monolayer of well-ordered molecules is

View Article Online
DOI: 10.1039/C8NR02069H

characterized by a complex organization. Analysis of the CB9CB monolayer shows a number of the characteristic features. The first one are paired bright spots ordered in a face to face position in periodically occurring rows (these linear elements of the surface are marked by (1) in Fig. 6a and by white arrows in Fig. 6b). The area between these rows is characterized by a very dense packing of bright spots – indicating that the structure is made up by interlocked molecules. These areas are characterized by significantly different STM contrast. This is clearly visible in the larger-area image (Fig. 6a) where bands of lower and higher brightness are marked with (2) and (3), respectively. In general, the different brightness in the STM image can be the result of two factors: the real geometry, as the bright area is simply thicker and its surface is located higher (closer to the STM tip), or this can be due to locally occurring differences in the electrical conductivity in the direction perpendicular to the layer surface. Despite this ambiguity concerning the origin of the observed effect, in both cases a higher density of cyanobiphenyl units is expected in the brighter band (3). These characteristic surface features, supported by more detailed analyses of the images recorded at higher resolution (Figs 6b and 8a) enabled us to determine the CB9CB monolayer unit cell parameters: a = 7.8 nm b = 2.6 nm γ = 93° (the unit cell is marked in the images by white rectangle). We note that the largest unit cell dimension (parameter a) is more than two and half times larger than the molecule size along its longitudinal axis. The parameter b of the unit cell corresponds to a separation between every second set of paired spots in the characteristic rows (1). This is because two adjacent paired spots are not fully equivalent in the STM images, their surrounding and relative positions are slightly different (see Figs 6b and 8a). The separation between two adjacent paired spots in the rows (1) is 1.3 nm. This suggests that the crystallographic unit cell for this structure must consist of several molecules. Due to the complex organization of CB9CB molecules in the monolayer, it is difficult to propose a model for the adsorption geometry based solely on the STM images. Hence we use XRD data obtained for 3D single crystals of the same molecules to identify the structure of the assembly. Specifically correlations between the 2D (monolayer) and 3D crystal structure are important. According to Hori et al.[22] and the corresponding data deposited in Cambridge Structural Data Base (CCDC225581-225584) single crystals of CB9CB are characterized by a trigonal unit cell (space group $P3_121$) yielding the following crystallographic parameters: a =

View Article Online
DOI: 10.1039/C8NR02069H

0.9159 nm, *b* = 0.9159 nm, *c* = 8.7318 nm, α = 90º, β = 90º, γ = 120º, Z=9. The authors suggest that the complex supramolecular organization with three fold symmetry axis is a consequence of a coexistence and mutual interactions of dimers in two different conformations in the 3D crystals that vary in the numbers and positions of twists in the spacer chain. The asymmetric conformer has one twisted moiety located at one side of the chain whereas in the case of the symmetric conformer the twisted moieties are located at both its ends. This diversity of molecular conformations and the resulting complex supramolecular features are unique and distinguishes the odd dimers from the even ones that form a simple layer crystal. We note that the projections of the 3D structure on planes parallel to the *c* axis, that is 3-fold axis of the structure, indicate clear similarities with the organization of the same molecules in the monolayer. This correlation includes the crystallographic unit cell dimensions: *c* being 8.7 nm and 7.8 nm in the crystal and the monolayer, respectively, as well as the similarity in *b* dimension 0.9 nm and 1.3 nm, in the crystal and the monolayer respectively. This takes into account half of the unit cell dimension corresponding to the separation between paired spots in the monolayer. To clarify whether the features observed by STM correlate fully with the XRD data the following procedure was performed for several planes parallel to the *c* axis. First, the position of each phenyl ring in the crystal structure of the plane was marked by a circle. An example of the results obtained for (100) plane is presented in Fig. 7a (white and black circles correspond to phenyl units of dimers with asymmetric and symmetric conformations, respectively). Then, considering all phenyl rings originating from molecules in both conformations as indistinguishable, the obtained organization was multiplied over a larger area. Careful analysis, performed for several crystallographic planes, indicates that only in the case of (100) plane a good correlation between the 2D distribution of phenyl rings in the single crystal (Fig. 7b) and the STM images of the monolayer (Figs 6, 8) can be obtained. This is clearly shown when we focus on the distribution of larger black spots in this plane consisting of four circles, i.e. four phenyl rings aggregates from two adjacent molecules. All characteristic features of the monolayer discussed above are also present in the single crystal, such as: i) characteristic rows of paired spots (1), and ii) two distinct areas between the rows, having lower (2) and higher (3) density of the phenyl rings. These parts correspond in the STM images of the monolayer to alternatively occurring darker (2) and

View Article Online
DOI: 10.1039/C8NR02069H

brighter (3) parallel bands. Moreover, carful inspection lead to the identification of further detailed similarities (see Fig. 8). The distribution of biphenyl units in the (100) plane of the single crystal, in the area between the characteristic rows of paired spots (paired spots are marked by (1) in scheme (b)) indicates the existence of a linear set of three aggregates (marked in the scheme as (a), (b) and (c)), each one consisting of four phenyl rings. This arrangement is clearly confirmed for the monolayer by the corresponding three bright spots in more resolved STM image (Fig. 8a). This shows that in monolayers the helical arrangement of molecules, detected for the crystal structure, is preserved.

Fig. 9 shows images of a monolayer formed by dimers with a longer spacer consisting of eleven methylene groups (CB11CB). The unit cell parameters determined for this monolayer are: a = 8.1 nm, b = 1.8 nm, $\gamma = 94°$. When compared to the shorter dimer, the longitudinal dimension of the unit cell (parameter a) of this larger adsorbate is extended due to the spacer elongation. We note that the unit cell parameter in these systems is very close to that found by carbon k-edge experiments[28] confirming thus the structural model with detailed molecular level information. However, there are two additional interesting features in the STM images. There seems to be same organization of the bright spots in the STM images between the characteristic rows in the monolayer which determine short axis b of the unit cell. There is a linear set of three larger spots (marked by white arrows in Fig. 9b), located on one side of this area (i.e. in part of higher density of phenyl rings). Another observation is connected with the evolution of the shorter - b dimension of the unit cell, caused by the extension of the spacer length in the series of odd membered dimers. For the dimer with the shortest spacer (CB7CB) a windmill-like organization was observed indicating the formation of a bent conformation on the substrate surface and a tendency of four molecules to form aggregates. An increase of the spacer chain length leads to more complex supramolecular organization due to stronger intermolecular interactions (*vide supra* for its description). This is clearly evidenced by a decrease of the shorter dimension of the unit cell with increasing spacer length (from 2.6 nm (CB9CB) to 1.8 nm (CB11CB). Due to slightly different contrast in the STM image this dimension corresponds to the separation between every second spot pair in the characteristic rows of the

View Article Online
DOI: 10.1039/C8NR02069H

monolayer. As a consequence the corresponding separation between the adjacent paired spots in the rows determined for CB9CB in the monolayer (1.3 nm) is larger when compared to the corresponding distance in the single crystal (0.9 nm). However, upon extension of the spacer to an undecyl unit the separation in the monolayer drops to the value typical for the 3D organization (c.a. 0.9 nm).

We assume that a windmill like organization of the longer odd spacered systems is disfavored, as the packing density decreases with increasing spacer length. Interdigitated structures seem to be the most efficient packing mode for these molecules, mirroring thus the packing the in N_{TB} phase.

3.3. Comparison of supramolecular organization of symmetrical and asymmetrical derivatives

STM images of monolayers formed by symmetrical (CB9CB) and non-symmetrical (CB9DFCB) molecules are compared in Fig. 10. The unit cell parameters, determined from STM measurements of the asymmetric molecules monolayer, are: a = 7.4 nm, b = 2.4 nm, γ = 91°. These values are comparable to those obtained for the CB9CB dimer. Moreover, the same typical elements of this complex monolayer organization can be distinguished, such as: i) characteristic rows of paired bright spots (marked by white arrows), and ii) areas of higher and lower conductivity between these rows (evidenced by brighter and darker parts of the image). It can therefore be concluded that both molecules exhibit the same type of the complex supramolecular organization with helical arrangement of molecules. Careful inspection of the images of both dimers, symmetric CB9CB and asymmetric CB9DFCB, seems to indicate that the monolayer of the asymmetric derivative, being larger in size, is characterized by a slightly smaller unit cell. This effect can be ascribed to the presence of two strongly electronegative fluorine atoms in the asymmetrical molecule. Strong intermolecular hydrogen bonds, resulting in denser molecular packing are therefore expected in the monolayer of this derivative. The second noticeable difference is associated with the local distribution of the bright spots within the unit cell area (see corresponding zoom images, in which four corners of the unit cell are marked by white circles). The observed dissimilarities can be

View Article Online
DOI: 10.1039/C8NR02069H

rationalized by two general factors: i) a slightly different organization and association of mesogenic units in the monolayers of both molecules, caused by their different chemical structure, and/or ii) different submolecular STM contrast mainly resulting from the presence or absence of strongly electronegative fluorine atoms. The subtle differences in the assembly behavior of the symmetric and non-symmetric dimers highlight the need for further detailed and systematic investigations.

4. Conclusions

STM investigations of a series of six cyanobiphenyls bimesogens enabled us to analyze the evolution of their 2D supramolecular organization on a HOPG substrate induced by the length of the flexible alkyl spacer. The results can be summarized as follows:

- 2D supramolecular organization of the examined dimers is strongly influenced by the number and parity of methylene groups in the spacer;
- Dimers with shorter spacers (consisting of 7 and 8 methylene groups) exhibit similar 2D supramolecular structures, two types of differently ordered monolayers are formed: either *via* dense packing, wherein the molecules are oriented in one direction and ordered into parallel rows (layer structure), or *via* a less dense packing, the dimers are organized into a chiral windmill-like structure.
- The effect of the spacer on the resulting supramolecular organization of the investigated dimers becomes more pronounced with increasing length. For derivatives with longer alkyl chains, ranging from 9 to 12 methylene groups a very different organization is observed, depending on the parity of carbon atoms in the chain (even *versus* odd). Even membered dimers (CB10CB, CB12CB) are organized in a layer structure, *i.e.* the same as observed for molecules with shorter spacers. The difference in the unit cell in the longitudinal dimension can be directly correlated with the length of the molecules.
- Odd-membered dimers (CB9CB, CB11CB) exhibit a much complex 2D supramolecular organization with a helical arrangement of the molecules. The observed structure of the

View Article Online
DOI: 10.1039/C8NR02069H

monolayer can be considered as a complex arrangement of molecular pairs rather than individual molecules. This organization is characterized by much larger unit cells in comparison to those determined for even membered dimers. The discussion and interpretation of STM images obtained for odd-membered molecules was possible by comparison with the organization of the same molecules in single crystals derived from XRD analysis.[22] This comparison firmly confirms a good correlation between the supramolecular organization of molecules in the monolayer and in one of the crystallographic planes of the 3D single crystals. The model for the organization, using molecular level resolution is very similar to that proposed for these molecules in the N_{TB} phase. Interdigitation of the bent and twisted molecules increases packing density leading to unit cell parameters with values similar to those detected for the helical pitch in the N_{TB} phase.

Conflicts of interest

There are no conflicts of interest to declare.

Acknowledgments

This work was financially supported by the National Science Centre (Poland) through a Research Project OPUS No. 2015/17/B/ST4/03845 granted for years 2016 – 2019. Z.A. and C.W. acknowledge funding through the EPSRC (EP/M015726 and EP/J004480). E.G. and D.P. acknowledge the support of the National Science Centre (Poland) through a Research Project No. 2016/22/A/ST5/00319.

View Article Online
DOI: 10.1039/C8NR02069H

References

1. R. A. Street, *Nature Materials,* 2006, **5**, 171.

2. P. J. Barnes, A. G. Douglass, S. K. Heeks and G. R. Luckhurst, *Liq. Cryst.,* 1993, **13**, 603.

3. V. P. Panov, M. Nagaraj, J. K. Vij, P. Panarin, A. Kohlmeier, M. G. Tamba, R. A. Levis and G. H. Mehl, *Phys. Rev. Lett.,* 2010, **105**, 167801.

4. V. P. Panov, R. Balachandran, M. Nagaraj, J. K. Vij, M. G. Tamba, A. Kohlmeier and G. H. Mehl, *Appl. Phys. Lett.,* 2011, **99**, 261903.

5. D. Chen, J. H. Porada, J. B. Hooper, A. Klittnick, Y. Shen, M. R. Tuchband, E. Korblova, D. Bedrov, D. M. Walba, M. A. Glaser, J. E. Maclennan and N. A. Clark, *Proc. Natl. Acad. Sci. U.S.A.,* 2013, **110**, 15931.

6. C. Meyer, G. R. Luckhurst and I. Dosov, *Phys. Rev. Lett.,* 2013, **111**, 067801.

7. S. M. Jansze, A. Martinez-Felipe, J. M. D. Storey, A. T. M. Marcelis and C. T. Imrie, *Angew. Chem., Int. Ed.* 2015, **54**, 643.

8. R. B. Meyer, in Les Houches Summer School in Theoretical Physics, ed. R. G. Balian and G. Weil, Gordon and Breach, New York 1976, pp. 273.

9. I. Dozov, *Europhys. Lett.,* 2001, **56**, 247.

10. M. Cestari, S. Diez-Berart, D. A. Dunmur, A. Ferrarini, M. R. de la Fuente, D. J. B. Jackson, D. O. Lopez, G. R. Luckhurst, M. A. Perez-Jubino, R. M. Richardson, J. Salud, B. A. Timimi and H. Zimmermann, *Phys. Rev. E: Stat. Nonlinear, Soft Matter Phys.,* 2011, **84**, 031704.

11. P. A. Henderson and C. T. Imrie, *Liq. Cryst.,* 2011, **38**, 1407.

12. R. J. Mandle, E. J. Davis, C. T. Archbold, S. J. Cowling and J. W. Goodby, *J. Mater. Chem. C,* 2014, **2**, 556.

13. N. Sebastian, D. O. Lopez, B. Robles-Hernandez, M. R. de la Fuente, J. Salud, M. A. Perez-Jubindo, D. A. Dunmur, G. R. Luckhurst and D. J. B. Jackson, *Phys. Chem. Chem. Phys.,* 2014, **16**, 21391.

14. R. J. Mandle, E. J. Davis, C. T. Archbold, C. C. A. Voll, J. L. Andrews, S. J. Cowling and J. W. Goodby, *Chem. – Eur. J.,* 2015, **21**, 8158.

15. E. Gorecka, N. Vaupotic, A. Zep, D. Pociecha, J. Yoshioka, J. Yamamoto and H. Takezoe, *Angew. Chem., Int. Ed.,* 2015, **54**, 10155.

View Article Online
DOI: 10.1039/C8NR02069H

16. C. T. Archbold, R. J. Mandle, J. L. Andrews, S. J. Cowling and J. W. Goodby, *Liq. Cryst.,* 2017, **44**, 2079.

17. Y. Wang, G. Singh, D. M. Agra-Kooijman, M. Gao, H. K. Bisoyi, C. Xue, M. R. Fisch,; S. Kumar and Q. Li, *Cryst. Eng. Comm.,* 2015, **17**, 2778.

18. A. Al-Janabi, R. J. Mandle and J. W. Goodby, *RSC Adv.,* 2017, **7**, 47235.

19. D. Chen, M. Nakata, R. Shao, M. R. Tuchband, M. Shuai, U. Baumeister, W. Weissflog, D. M. Walba, M. A. Glaser, J. E. Maclennan and N. A. Clark, *Phys. Rev. E: Stat., Nonlinear, Soft Matter Phys.,* 2014, **89**, 022506.

20. S. P. Sreenilayam, V. P. Panov, J. K. Vij and G. Shanker, *Liq. Cryst.,* 2017, **44**, 244.

21. C. T. Imrie and G. R. Luckhurst, *J. Mater. Chem.,* 1998, **8**, 1339.

22. K. Hori, M. Iimuro, A. Nakao and H. Toriumi, *J. Mol. Structure,* 2004, **699**, 23.

23. R. Balachandran, V. P. Panov, Y. P. Panarin, J. K. Vij, M. G. Tamba, G. H. Mehl and J. K. Song, *J. Mater. Chem. C,* 2014, **2**, 8179.

24. Ch.-J. Yun, M. R. Vengatesan, J. K. Vij and J.-K. Song, *Appl. Phys. Lett.,* 2015, **106**, 173102.

25. D. A. Paterson, M. Gao, Y.-K. Kim, A. Jamali, K. L. Finley, B. Robles-Hernandez, S. Diez-Berart, J. Salud, M. Rosario de la Fuente, B. A. Timimi, H. Zimmermann, C. Greco, A. Ferrarini, J. M. D. Storey, D. O. Lopez, O. D. Lavrentovich, G. R. Luckhurst and C. T. Imrie, *Soft Matter,* 2016, **12**, 6827.

26. R. You, D. A. Paterson, J. M. D. Storey, C. T. Imrie and D. K. Yoon, *Liq. Cryst*., 2017, **44**, 168.

27. S. M. Salili, M. G. Tamba, S. N. Sprunt, C. Welch, G. H. Mehl, A. Jákli and J. T. Gleeson, *Phys. Rev. Lett.,* 2016, **116**, 217801.

28. C. Zhu, M. R. Tuchband, A. Young, M. Shuai, A. Scarbrough, D. M. Walba, J. E. Maclennan, C. Wang, A. Hexemer and N. A. Clark, *Phys. Rev. Lett.,* 2016, **116**, 147803.

29. M. Salamończyk, N. Vaupotič, D. Pociecha, C. Wang, C. Zhu, and E.Gorecka, *Soft Matter,* 2017, **13**, 6694.

30. W. D. Stevenson, Z. Ahmed, X. B. Zeng, C. Welch, G. Ungar and G. H. Mehl, *Phys. Chem. Chem. Phys.,* 2017, **19**, 13449.

31. C. T. Imrie and P. A. Henderson, *Chem. Soc. Rev.,* 2007, **36**, 2096.

32. R. J. Mandle, *Soft Mater,* 2016, **12**, 7883.

View Article Online
DOI: 10.1039/C8NR02069H

33. R. J. Mandle, *Chem. Eur. J.,* 2017, **23**, 8771.

34. V. P. Panov, J. K. Vij and G. H. Mehl, *Liq. Cryst.,* 2017, **44**, 147.

35. J. Zapala, M. Knor, T. Jaroch, A. Maranda-Niedbala, E. Kurach, K. Kotwica, R. Nowakowski, D. Djurado, J. Pecaut, M. Zagorska and A. Pron, *Langmuir,* 2013, **29**, 14503.

36. T. Jaroch, A. Maranda-Niedbała, M. Góra, J. Mieczkowski, M. Zagórska, M. Salamończyk, E. Górecka and R. Nowakowski, *Synth. Metals,* 2015, **204**, 133.

37. K. Walzer and M. Hietschold, *J. Vac. Sci. & Technol. B,* 1996, **14**, 1461.

38. D. P. E. Smith, J. K. H. Horber, G. Binnig and H. Nejoh, *Nature,* 1990, **344**, 641.

39. T. Kadotani, S. Taki, H. Okabe and S. Kai, *Jpn J. Appl. Phys.,* 1996, **35**, L1345.

40. T. Kadotani, S. Taki and S. Kai, *Jpn. J. Appl. Phys.,* 1997, **36**, 4440.

41. S. Taki, S. Sagara, T. Kadotani and S. Kai, *J. Phys. Soc. Jpn.,* 1999, **68**, 709.

42. S. Taki and S. Kai, *Jpn. J. Appl. Phys.,* 2001, **40**, 4187.

43. E. Lacaze, M. Alba, M. Goldmann, J. P. Michel and F. Rieutord,

Eur. Phys. J. B, 2004, **39**, 261.

44. Z. Ahmed, C. Welch, G. H. Mehl, *RSC Advances*, 2015, 5, 93513.

45. Z. Ahmed, PhD thesis "The design, synthesis and properites of dimeric molecules exhibiting nematic-nematic transitions" University of Hull, November 2014.

46. M. Wilms, M. Kruft, G. Bermes and K. Wandelt, *Rev. Sci. Instrum.,* 1999, **70**, 3641.

47. C. Meyer, G. R. Luckhurst and I. Dozov, *J. Mater. Chem. C,* 2015, **3**, 318.

48. E. Gorecka, N. Vaupotic and D. Pociecha, *Chem. Mater.,* 2007, **19**, 3027.

View Article Online
DOI: 10.1039/C8NR02069H

Figure Captions

Fig. 1 Chemical formula of the studied molecules: (a) symmetric dimers - 1,ω-bis(4-cyanobiphenyl-4'-yl)n-alkanes (CBnCB, n=7-12), and (b) asymmetric difluoro-substituted derivative (CB9DFCB); (c) Schematic comparison of molecular shape of CBnCB containing two para linked mesogenic units with odd- (n=7) or even- (n=8) membered spacer.

Fig. 2 (a,c) STM images and (b) proposed adsorption geometry (layer structure) of monomolecular layers of CB7CB on HOPG. (b1) Schematic representation of intermolecular hydrogen bonds in the layer; (c1) Zoom image of (c); (a) 15 x 15 nm^2, (c) 15 x 7.5 nm^2, V_{bias} = 0.95 V, I_t = 1 nA.

Fig. 3 (a,b) STM images and (c) proposed adsorption geometry (layer structure) of monomolecular layers of CB8CB on HOPG; (a) 31 x 31 nm^2, (b) 15 x 15 nm^2, V_{bias} = 1 V, I_t = 1 nA.

Fig. 4 STM images of monomolecular layers (windmill-like structure) of (a) CB7CB and (c) CB8CB on HOPG. (b) Proposed adsorption geometry of corresponding CB7CB monomolecular layer; (a, c) 15 x 15 nm^2, V_{bias} = 1 V, I_t = 0.9 nA.

Fig. 5 (a) STM image and (b) proposed adsorption geometry of monomolecular layers of CB12CB on HOPG; (a) 15 x 15 nm^2, V_{bias} = 1 V, I_t = 1nA.

Fig. 6 STM images of CB9CB monomolecular layers on HOPG. Characteristic features of the monolayer: periodically occurring rows of double bright spots ordered in a face to face position, and bands between them of lower and higher brightness are marked in image (a) by (1), (2) and (3), respectively. Bright rows in image (b) indicate periodically occurring characteristic rows of double bright spots; (a) 46 x 46 nm^2, (b) 31 x 31 nm^2, V_{bias} = 1 V, I_t = 1 nA.

Fig. 7 Distribution of phenyl units in (100) plane of CB9CB crystal structure (white and black circles in (a) correspond to phenyl units of dimers with asymmetric and symmetric conformations, in large area scheme (b) all phenyl units are marked by black circles (considered as indistinguishable)). On the basis of crystal structure from Cambridge Structural Data Base (CCDC225581-225584).

Fig. 8 (a) STM image at higher magnification of CB9CB monomolecular layers on HOPG and (b) corresponding distribution of phenyl units in (100) plane of crystal structure (characteristic rows of double spots are marked by (1) while three aggregates between them, each one consisting of four phenyl rings, by (a), (b) and (c), respectively); (a) 15 x 15 nm^2, V_{bias} = 0.6 V, I_t = 1 nA.

View Article Online
DOI: 10.1039/C8NR02069H

Fig. 9 STM images of CB11CB monomolecular layers on HOPG (three aggregates of phenyl units between characteristic rows of double spots are marked by white arrows); (a) 31 x 31 nm^2, (b) 15 x 15 nm^2, V_{bias} = 1 V, I_t = 1 nA.

Fig. 10 STM images of (a) CB9CB and (b) (CB9DFCB) monomolecular layers on HOPG (characteristic rows of double spots are marked by white arrows); (a,b) 24 x 24 nm^2, V_{bias} = 1 V, I_t = 1 nA.

View Article Online
DOI: 10.1039/C8NR02069H

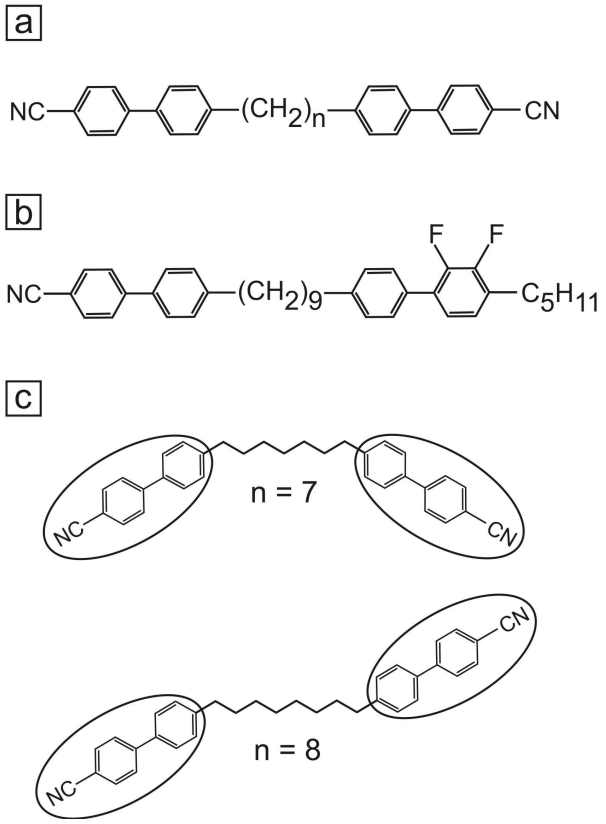

Figure 1

View Article Online
DOI: 10.1039/C8NR02069H

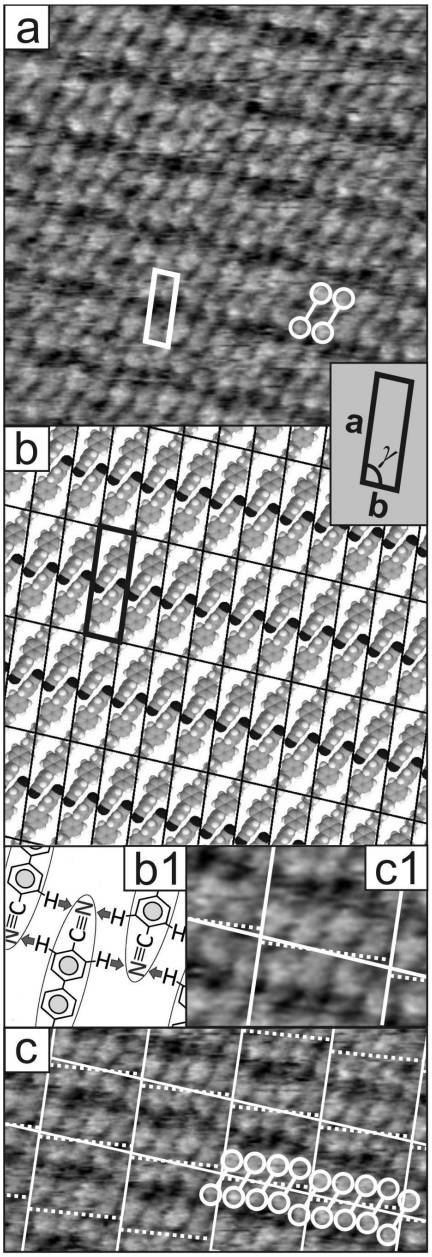

Figure 2

View Article Online
DOI: 10.1039/C8NR02069H

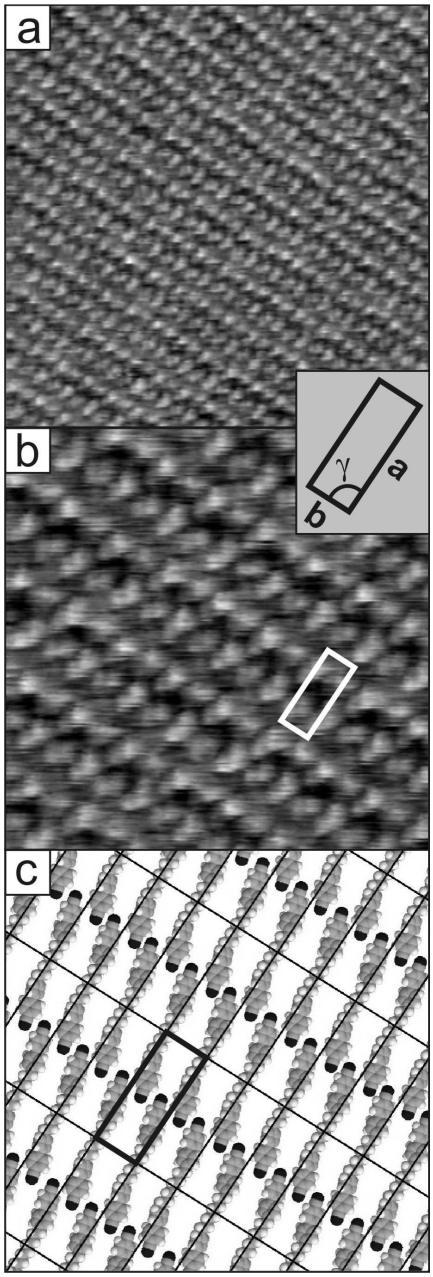

Figure 3

View Article Online
DOI: 10.1039/C8NR02069H

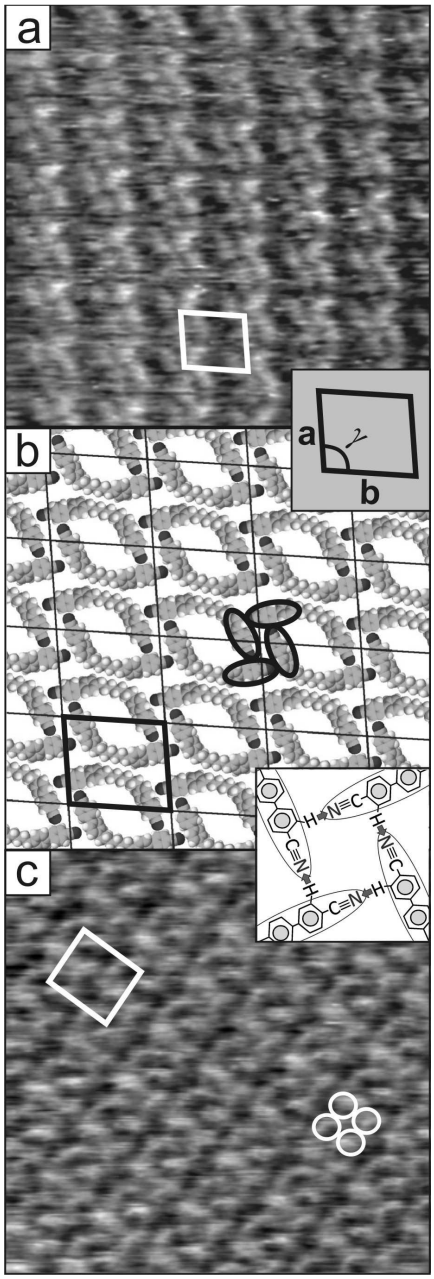

Figure 4

View Article Online
DOI: 10.1039/C8NR02069H

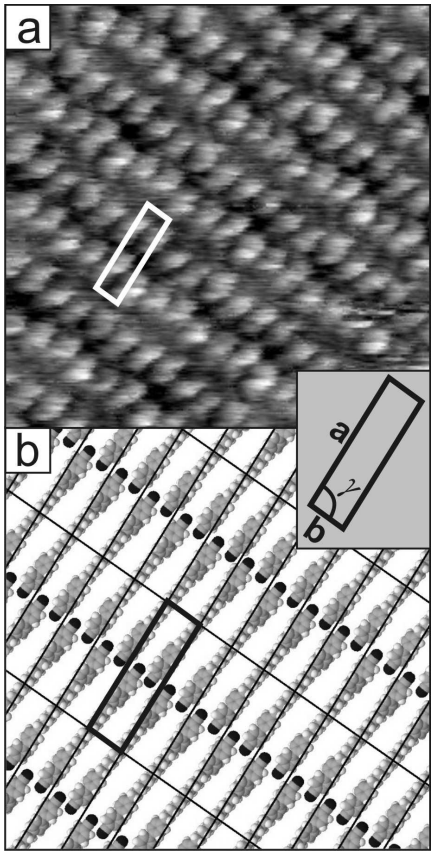

Figure 5

View Article Online
DOI: 10.1039/C8NR02069H

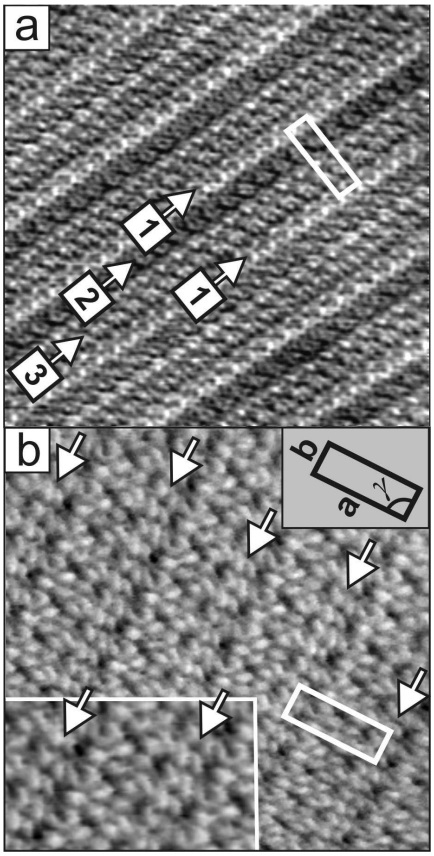

Figure 6

View Article Online
DOI: 10.1039/C8NR02069H

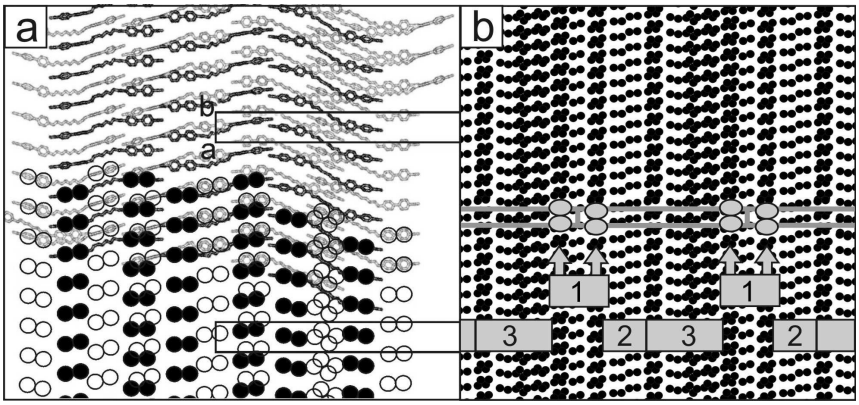

Figure 7

View Article Online
DOI: 10.1039/C8NR02069H

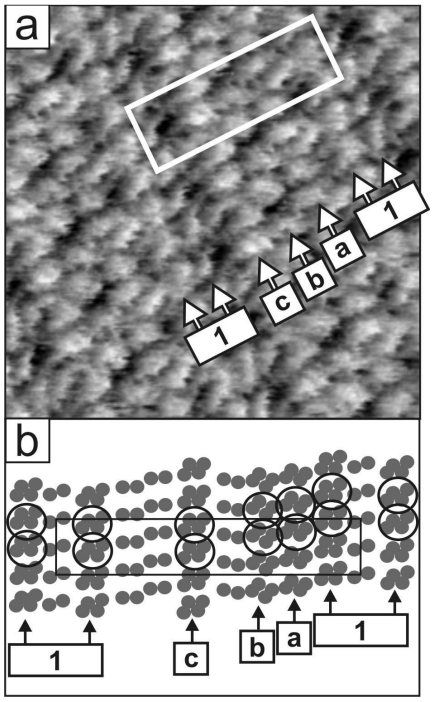

Figure 8

View Article Online
DOI: 10.1039/C8NR02069H

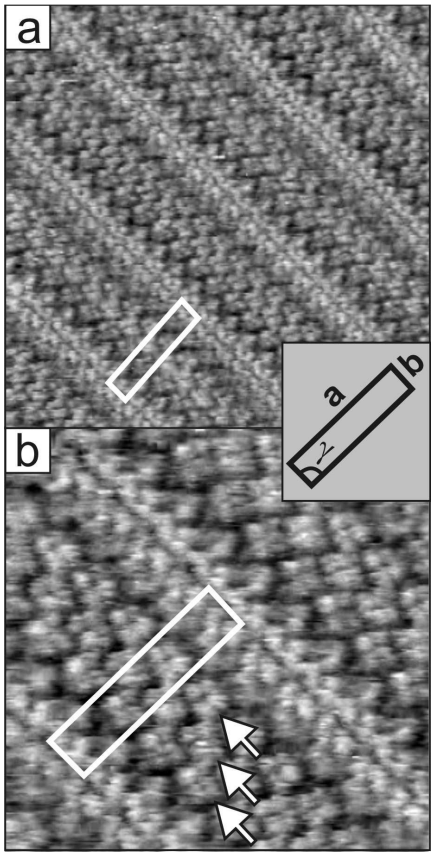

Figure 9

View Article Online
DOI: 10.1039/C8NR02069H

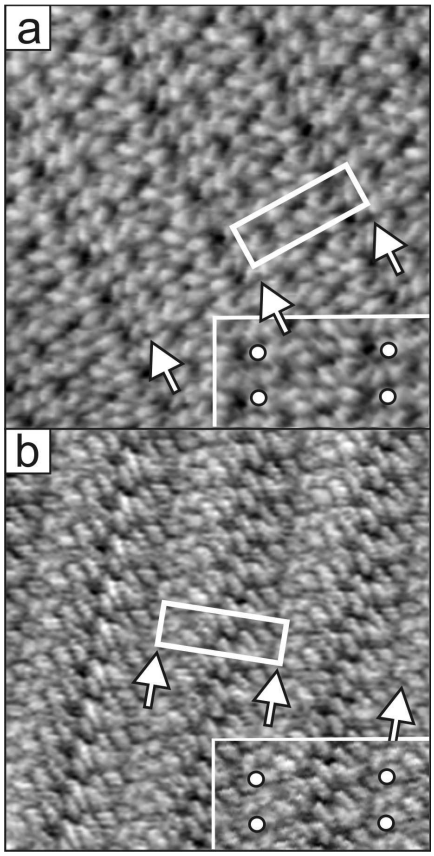

Figure 10

View Article Online
DOI: 10.1039/C8NR02069H

"Supramolecular organization of liquid-crystal dimers - bis-cyanobiphenyl alkanes on HOPG by scanning tunneling microscopy" by K. Krzyżewska et al.

Table of Contents Entry

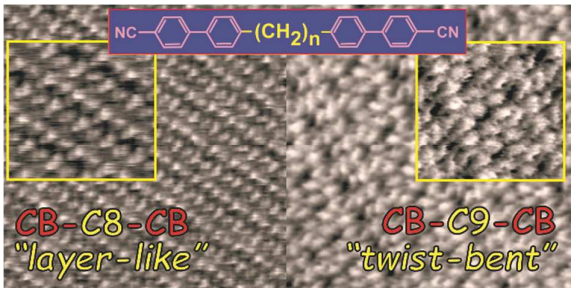

Effect of the alkyl spacer length on 2D self-organization of cyanobiphenyls bimesogens on HOPG is studied by scanning tunneling microscopy